A generalization of Distinct Element Method to tridimensional particles with complex shapes

Lionel Pournin & Thomas. M. Liebling
EPFL - Ecole Polytechnique Fédérale de Lausanne, Mathematics Institute, Lausanne, Switzerland

The distinct element method was originally designed to handle spherical particles. Here, this method is generalized to a wider range of particle shapes called *spherosimplices*. A contact detection method is given as well which uses weighted Delaunay triangulations to detect contacts occurring in a population of particles with such shapes. Finally, a set of numerical experiments is performed indicating that the overall contact detection complexity is linear in the number of particles.

1 INTRODUCTION

The distinct element method (DEM) is widely used to perform granular media simulations. The two key elements this requires are an adequate model for inter-particulate contact forces and an efficient contact detection method. Although this method originally handles granular media composed of spherical particles, making it possible to process non-spherical particles has turned out to be of utmost importance. Indeed it is such grains that one finds in nature and many important phenomena cannot be reproduced just using spherical grains. Here, we propose a generalization of the distinct element method to a wide range of non-spherical particles. In the following, we describe some of the shapes this generalization will be able to work with and explain how the contact force models should be handled. Then, we address the question of detecting contacts between pairs of such particles, by generalizing the method described in (Ferrez and Liebling 2002) which relies on the properties of the weighted Delaunay triangulations to detect contacts in the spherical particles case.

2 PARTICLE SHAPES AND CONTACT MODELING

From here on, a particle P will be the Minkowski sum of a simplex s (either a point, a line segment, a triangle or a tetrahedron) with a ball of radius r centered at the origin. We say s is the skeleton of P and r its radius. Those particles, shown on figure 1 will appropriately be called *spherosimplices*, or depending on their skeletons *spherosegments* (also called spherocylinders (Pournin et al. 2005)), *spherotriangles* and *spherotetrahedra*.

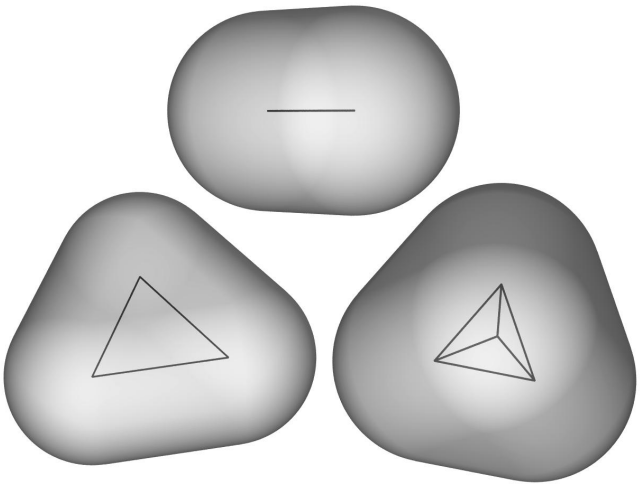

Figure 1: The three non-spherical *spherosimplices* used to model particle shapes, together with their skeletons.

These shapes are special cases of more general structures (not necessarily convex *spheropolyhedra*) which we can also treat, and which we will discuss elsewhere. Two particles P and Q are in contact whenever they overlap, that is if $P \cap Q \neq \emptyset$. The overlapping between P and Q models the deformation at the contact point.

In the original distinct element method, that is when P and Q are spheres, the amount of overlapping at the contact point is quantified by the *normal overlap* ξ_n as :

$$\xi_n = r_P + r_Q - \|s_Q - s_P\|, \tag{1}$$

where s_P and s_Q are the centers of P and Q respectively and r_P and r_Q are their radii (see figure 2). A

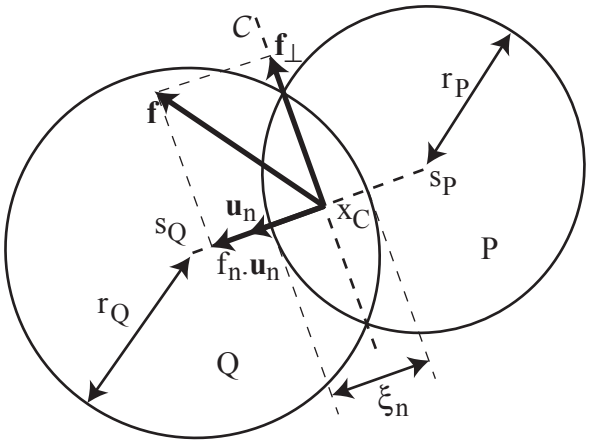

Figure 2: Geometrical modeling of a contact between spherical particles P and Q in the usual DEM framework with the contact force $\boldsymbol{f}$ applied by particle P on particle Q.

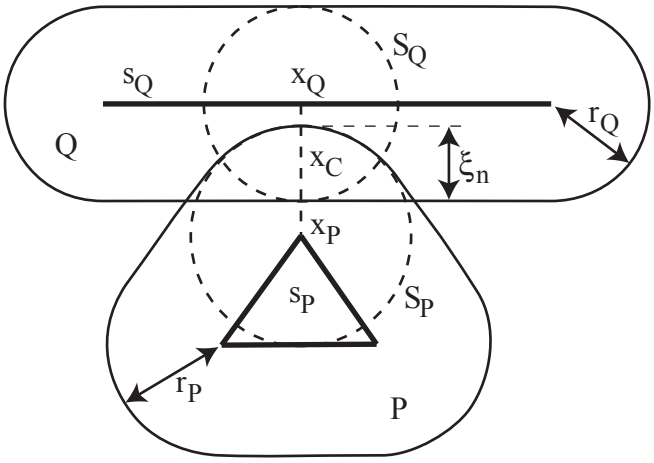

Figure 3: Geometrical modeling of a contact between non-spherical particles P and Q (here, a spherotriangle and a spherosegment). According to the model, x_P and x_Q are points in s_P and s_Q so that $\|x_Q - x_P\|$ is minimal and the contact between P and Q has same ξ_n, $\boldsymbol{u}_n$ and x_C as the imaginary contact between spheres S_P and S_Q.

unit vector $\boldsymbol{u}_n$ normal to the contact area can be defined as $\boldsymbol{u}_n = \frac{s_Q - s_P}{\|s_Q - s_P\|}$. A force $\boldsymbol{f}$ is applied on the particles at contact point accordingly to the third Newton law (that is $\boldsymbol{f} = \boldsymbol{f}_{P\to Q} = -\boldsymbol{f}_{Q\to P}$) and its normal component $f_n = \boldsymbol{f}.\boldsymbol{u}_n$ will be given as a function of ξ_n and its time derivative $\dot{\xi}_n$. The most popular model for this contact force, first introduced in (Cundall and Strack 1979) reads :

$$f_n = k_n \xi_n + c_n \dot{\xi}_n \tag{2}$$

The parameters k_n and c_n depend on the geometrical and mechanical properties of the contacting spheres (Pournin et al. 2002). Other expressions for $\boldsymbol{f}_n$ have been proposed in (Walton and Braun 1986; Pournin et al. 2002). The point x_C on either P and Q to which the total contact force is effectively applied is the intersection of segment $[s_P, s_Q]$ with the plane $\mathcal{C}$ containing the circular intersection of the boundaries of P and Q. A *tangential overlap* $\boldsymbol{\xi}_\perp$ accounting for the tangential deformation at sticky contacts can be defined as well by integrating the tangential relative speed of P and Q at the contact point x_C. The tangential component $\boldsymbol{f}_\perp = \boldsymbol{f} - f_n \boldsymbol{u}_n$ of the contact force can therefore be modeled from $\boldsymbol{\xi}_\perp$ the same way $\boldsymbol{f}_n$ has been from ξ_n. This tangential force can be bounded according to Coulombian friction law in order to account for slippery contacts.

Now, if P and Q are not necessarily spherical, let x_P and x_Q be the points in s_P and s_Q respectively so that $\|x_Q - x_P\|$ is minimal (see figure 3). Of course there may be several such pairs in degenerate cases, for example when s_P and s_Q are two parallel triangles, but then x_P (resp. x_Q) should be chosen as the barycenter of the possible points on s_P (resp. s_Q) which provides an easy, yet intuitive solution. A normal overlap, a unit vector normal to the contact area and a contact point can be defined in this general case by replacing s_P and s_Q by x_P and x_Q in the spherical case definitions of those quantities. This actually amounts to considering that the contact between P and Q actually occurs between the sphere S_P of radius r_P centered at point x_P and the sphere S_Q of radius r_Q centered at point x_Q.

The contact point x_C (to which the contact force is applied) will therefore be the intersection of segment $[x_P, x_Q]$ with the plane $\mathcal{C}$ containing the circular intersection of the boundaries of S_P and S_Q, the overlap ξ_n will read :

$$\xi_n = r_P + r_Q - \|x_Q - x_P\|, \tag{3}$$

and $\boldsymbol{u}_n$ will read $\boldsymbol{u}_n = \frac{x_Q - x_P}{\|x_Q - x_P\|}$. The normal component of the contact force should then be computed from ξ_n according to (2) or to any other contact force model. Besides, the knowledge of x_C allows the computation of $\boldsymbol{\xi}_\perp$ by integration of the tangential relative speed of P and Q at point x_C and $\boldsymbol{f}_\perp$ will be found from $\boldsymbol{\xi}_\perp$ following an appropriate force model. Once the forces and their application points are known, the velocities, spins and trajectories of the particles are obtained by integration of the usual motion equations. This requires that the inertia matrix of every particle be known. While those matrices have analytical expressions for all spherosimplices, we do not reproduce them here.

3 A TRIANGULATION-BASED CONTACT DETECTION METHOD

When simulating large populations of particles, an efficient contact detection method is required. Indeed, the quadratic complexity of testing all possible pairs of particles for contact quickly becomes prohibitive when the number of particles increases. This section focuses on adapting to our particular non-spherical shapes the triangulation-based method introduced in (Müller 1996; Ferrez and Liebling 2002) in the spherical case. The weighted Delaunay triangulation D

generated by a number of spheres S_1, ..., S_n centered at points x_1, ..., x_n is a particular mesh of the convex hull of $\{x_1, ..., x_n\}$ whose basic elements are tetrahedra. Its regularity properties are greatly appreciated particularly when it comes to numerically solving spatial differential equations. Furthermore, one of its properties turns to be useful for our contact detection concerns : *if two spheres S_i and S_j, $i \neq j$ intercept, then the segment $[x_i, x_j]$ is an edge of D*. Detecting contacts among the spherical particles P_1, ..., P_n then amounts to building the weighted Delaunay triangulation generated by P_1, ..., P_n and testing for contact the pairs of particles which are linked by an edge of D. Considering that in our practical cases the number of edges of D is linear in the number n of generating spheres (see section 4), this method allows to reduce the complexity of contact detection from $O(n^2)$ to $O(n)$, which is about the best one can hope for in this context. Of course, building and handling the weighted Delaunay triangulation requires special attention, but this issue will not be addressed here and one may refer to (Ferrez 2001) for more details.

Now, suppose P_1, ..., P_n are non-spherical particles with skeletons s_1, ..., s_n and radii r_1, ..., r_n. The triangulation based contact detection method can be adapted to those non-spherical particles as follows. Assign to each particle P_i a set Σ_i of spheres having no relative motion with respect to P_i and so that the two following conditions are satisfied :

Covering Condition : The point-wise union of the spheres in Σ_i contains P_i for all $i \in \{1, ..., n\}$.

Orthogonality Condition : Independently of the relative position of any two particles P_i and P_j, $i \neq j$, for two spheres $S_i \in \Sigma_i$ and $S_j \in \Sigma_j$ with radii R_i and R_j and centers x_i and x_j respectively, $\|x_i - x_j\|^2 > R_i^2 + R_j^2$.

If the covering condition is satisfied, the spheres in sets Σ_i are also called covering spheres. The orthogonality condition actually bounds the overlap of any two spheres assigned to different particles at any time during the simulation process. Calling D is the weighted Delaunay triangulation generated by the spheres in all Σ_i, $i \in \{1, ..., n\}$, provided the two above conditions are satisfied, the following holds : *if two particles P_i and P_j, $i \neq j$ intercept, then there exist two spheres $S_i \in \Sigma_i$ and $S_j \in \Sigma_j$ whose centers are linked by an edge of D.*

Therefore, detecting contacts among the non-spherical particles P_1, ..., P_n amounts to covering each particle with a set of spheres so that the orthogonality condition is satisfied, building the weighted Delaunay triangulation generated by those spheres and testing for contact those pairs of particles having at least one covering sphere each, whose centers are linked by an edge of D. A given pair of particles P_i and P_j will be in contact as soon as $r_i + r_j - \|x_j - x_j\| > 0$, where x_i and x_j are the points in S_i and S_j respectively so that $\|x_j - x_i\|$ is minimal as defined in previous section. The actual computation of x_i and x_j is a simple, yet interesting optimization problem (see (Pournin et al. 2005) for the case of two segments).

Covering the particles with spheres so that the orthogonality condition is satisfied may be done in a variety of ways. Here, we only address the simple case of identical regular spherotetrahedra, each being covered by a single sphere. Suppose P is such a spherotetrahedron with skeleton s and radius r. Call M its mass center and l the distance between M and any vertex of s. The covering sphere S of P will be centered at point M and its radius will be $l + r$ that is, just enough for it to cover P. In such a situation, the distance between M and the boundary of P is $l/3 + r$. This means that the smallest possible distance between the centers of two covering spheres equals $2l/3 + 2r - \xi_m$, where ξ_m is an upper bound to the overlaps which will occur at any contact throughout the simulation. Therefore, if $2l/3 + 2r - \xi_m \geq \sqrt{2}(l + r)$ then the orthogonality condition is satisfied. Recall that the overlap accounts for the deformation at the contact point. Hence, any realistic simulation should lead to small values for ξ_m/r. With the acceptable value of $\xi_m/r = 1/8$, we obtain that for $l \leq 0.61r$, the orthogonality condition is satisfied. These dimensions were used to produce some of the numerical experiments discussed in next section.

4 RESULTS AND DISCUSSION

The above generalization of the traditional distinct elements method allows investigating granular phenomena involving non-spherical particles. For spherosegments, granular crystallization (Pournin et al. 2005; Ramaioli et al. 2005) has been successfully replicated with our model, providing a first validation. Still, further validations are needed and numerical experiments with more complex shapes may be conducted such as shape segregation or granular stratification (Makse et al. 1997). This section only aims at giving a feeling about the complexity of the contact detection method.

Snapshots of experiments performed with this non-spherical version of the distinct element method are shown on figure 4. Those experiments consist in pouring particles into a cylindrical container of diameter 20 mm. This means that the number of particles gradually increases while the simulation performs. All particles have eight times the volume of a sphere of diameter 1 mm, independently of their shapes. Experiment 1 involves 250 spherosimplices of each kind. Experiment 2 involves 500 spheres and 500 spherotetrahedra, and experiments 3 and 4, 1000 spheroseg-

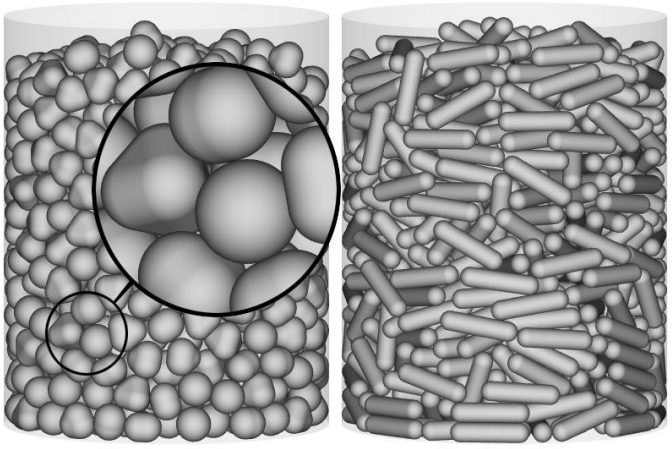

Figure 4: Snapshots of final states of numerical experiments. Left : experiment 1, right : experiment 3.

ments each.

For the first two experiments, each particle only uses one covering sphere for contact detection. This is achieved by calibrating every shape the same way the spherotetrahedra have been calibrated at the end of section 4. This constraint actually limits the particle's sharpness. Still, those particles are far from spherical and this way, the complexity of contact detection is the same as if all particles were spheres. In experiment 3, particles have an elongation coefficient l/r of 3, where l is half the length of the segment constituting their skeletons and r is their radius. With such elongated shapes, 5 covering spheres per particle are needed. In experiment 4, $l/r = 6$, and 9 covering spheres are needed for a particle. In every experiment, $\xi_m = 5 \times 10^{-5}$ m.

The computing time of the DEM process, including contact detection, is drawn on figure 5 against the number of simulated particles. In all cases it is almost linear. Observe that the slope of this linearity increases with particle elongation, naturally reflecting that the number of possible contacts is higher for elongated particles. The inset shows the number of edges of the triangulation, drawn versus the number of covering spheres and the four cases reveal identically linear. The slope of around 7 is close to the coordination number of random close-packed spheres, indicating that our method appropriately identifies the pairs of particles to be tested for contact.

5 CONCLUSION

This generalization of the distinct element method to non-spherical particles opens numerical simulation to a wide new range of granular media. Our linear triangulation-based contact detection method allows processing large populations of non-spherical particles. While many issues need to be further discussed, such as the influence of the shape of contact areas on the behaviour of a contact, the first trials to be found in (Pournin et al. 2005; Ramaioli et al. 2005) suggest that this model successfully captures the reality of non-spherical particles.

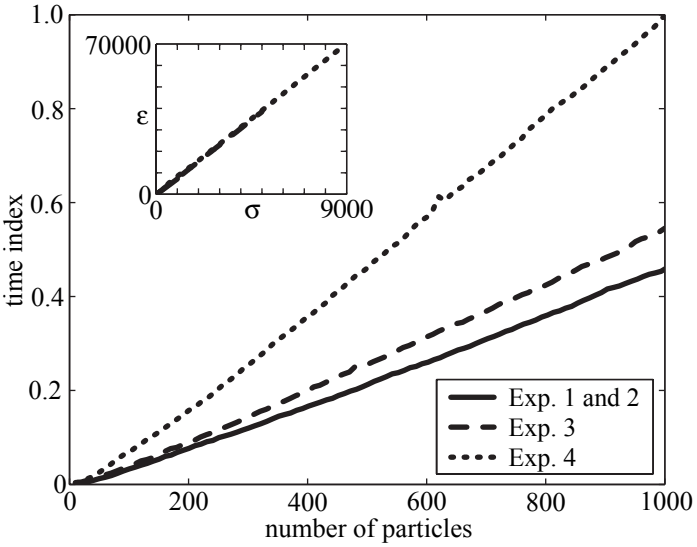

Figure 5: Actual computing time of the DEM process drawn versus the number of simulated particles for all experiments. The *time index* is normalized to 1 for 1000 of the last experiment's spherosegments. Each point is averaged over 400 DEM iterations. Inset : number ε of edges in the triangulation versus the number σ of covering spheres for the same experiments.

6 ACKNOWLEDGEMENTS

This project was funded by the Swiss National Science Foundation, grant # 200020-100499/1.

REFERENCES

Cundall, P. A. and O. D. L. Strack (1979). A discrete numerical model for granular assemblies. *Géotechnique 29*(1).

Ferrez, J.-A. (2001). *Dynamic Triangulations for Efficient 3D Simulation of Granular Materials*. Thèse N° 2432, EPFL.

Ferrez, J.-A. and T. M. Liebling (2002). Dynamic triangulations for efficient detection of collisions between sheres with applications in granular media simulations. *Philosophical Magazine B 82*(8), 905–929.

Makse, H. A., S. Havlin, P. R. King, and H. E. Stanley (1997). Spontaneous stratification in granular mixtures. *Nature 386*, 379–382.

Müller, D. (1996). *Techniques informatiques efficaces pour la simulation de mileux granulaires par des méthodes d'éléments distincts*. Thèse N° 1545, EPFL.

Pournin, L., T. M. Liebling, and A. Mocellin (2002). Molecular-dynamics force models for better control of energy dissipation in numerical simulations of dense granular media. *Phys. Rev. E 65*, 011302.

Pournin, L., M. Weber, M. Tsukahara, J.-A. Ferrez, M. Ramaioli, and T. M. Liebling (2005). Three-dimensional distinct element simulation of spherocylinder crystallization. *To appear in Granular Matter*.

Ramaioli, M., L. Pournin, and T. M. Liebling (2005). Numerical and experimental investigation of alignment and segregation of vibrated granular media composed of rods and spheres. In *Powders and Grains 2005*.

Walton, O. R. and R. L. Braun (1986). Viscosity, granular-temperature, and stress calculations for shearing assemblies of inelastic, frictional discs. *J. of Rheology 30*(949).